07

Enhanced laser pulse confinement in a photoconductive terahertz emitter through near-field sapphire-fiber microlens

© D.V. Lavrukhin[1], R.R. Galiev[1], N.V. Zenchenko[1], R.A. Khabibullin[1], V.N. Kurlov[2], Yu.G. Goncharov[3], K.I. Zaytsev[3], S.V. Garnov[3], D.S. Ponomarev[1,3]

[1] National Research Center „Kurchatov Institute“, Moscow, Russia
[2] Osipyan Institute of Solid State Physics RAS Russian Academy of Sciences, Chernogolovka, Moscow District, Russia
[3] Prokhorov Institute of General Physics, Russian Academy of Sciences, Moscow, Russia
E-mail: ponomarev_dmitr@mail.ru

Received May 23, 2025
Revised July 2, 2025
Accepted July 8, 2025

Near-field laser pulse confinement via specific sapphire-fiber microlens in a large-area photoconductive terahertz (THz) emitter is experimentally verified. We demonstrate that the proposed sapphire-fiber microlens provides a $\simeq$ 5-fold increase in emitted THz power, contributing to +6.5 dB in the signal-to-noise ratio and preserving the 2.5 THz spectral bandwidth.

Keywords: terahertz frequency, photoconductive antenna, THz emitter, sapphire fiber, near-field localization.

DOI: 10.61011/TPL.2025.10.62112.20384

Pulsed terahertz (THz) spectroscopy is progressing rapidly and is used to solve a wide range of fundamental and applied problems [1]. Among the existing designs of sources and detectors of THz pulses [2,3], optoelectronic (photoconductive) devices with excitation by femtosecond laser pulses are the ones used most often due to their simplicity, reliability, and flexibility (attributable to original electrode topologies). The low efficiency of conversion of laser excitation energy into THz radiation is one of the key incentives for research in this field.

We have proposed earlier to use shaped sapphire fiber (SSF) as an effective near-field microlens, which, under certain conditions [4], allows one to confine laser pumping near the edges of electrodes. In the present study, this approach was verified experimentally using the example of a large-area photoconductive (LAPC) emitter, which, unlike a conventional (i.e., single) source, generates THz radiation of increased power [5]; an original fixture for precise SSF positioning opposite the LAPC emitter electrodes was proposed. With laser pumping at a wavelength of 780 nm and an average power of just $P_{opt} = 20$ mW, the use of SSF provided a $\simeq$ 5-fold enhancement of power of generated THz radiation and helped increase the signal-to-noise ratio of the spectrometer by 6.5 dB with a spectral bandwidth of 2.5 THz.

Figure 1, *a* shows the LAPC emitter prototype with an original microlens based on SSF. SSF crystals with smooth lateral surfaces were grown in accordance with the Stepanov technique from a melt meniscus formed through a molybdenum matrix (edge-defined film-fed growth, EFG) [6]. Fiber diameter $d = 280\,\mu$m was chosen for the following engineering considerations. First, It is difficult to grow identical high-quality SSFs of a smaller diameter from melt. Second, fibers must be strong enough to withstand the process of assembly of LAPC emitter. Third, the width of a row of three-seven fibers must be comparable to the diameter of the laser excitation beam (at the $1/e^2$ power level), which is $\sim 1.5-2.0$ mm in the present case. The LAPC emitter chip featured five strip single THz emitters arranged in a row with paired electrodes 3.2 mm in length, gap $g = 20\,\mu$m, and a period of $350\,\mu$m. To suppress destructive interference of THz radiation from the electrodes of adjacent emitters in the far wave zone and reduce the dark current (leakage) in the low-temperature GaAs layer (low-temperature grown GaAs, LT-GaAs), a mesa structure was etched to separate adjacent emitters (see the inset in Fig. 2) [7]. SSF is placed above each emitter in the process of assembly, and the fixture with cells for its placement was fabricated using the simple and widely available 3D photopolymer printing method. The spatial resolution of photopolymer printing was $\Delta x \times \Delta y \times \Delta z = 35 \times 35 \times 30\,\mu$m. The pumped area of the LAPC emitter was $3.2 \cdot 10^{-3}$ cm^2. The fixture was designed so as to maintain a fixed distance between the fiber and the LAPC emitter surface (air gap $h_0 = 30\,\mu$m), which was confirmed by direct measurements with a micrometer. Special longitudinal and transverse marks between adjacent electrodes were formed by photolithography in order to align precisely the fibers in the fixture relative to the LAPC emitter chip. The estimated alignment error was $\sim 3-5\,\mu$m.

The power gain (K) was used as a quantitative measure of the influence of near-field focusing of laser excitation near the SSF/photoconductor interface on the generation of THz radiation in the LAPC emitter. Coefficient K was set by the ratio of integral excitation powers with and without fibers. As was noted above, the proposed design of the LAPC emitter with SSF features a thin air gap (h) between the bottom surface of the fiber and the

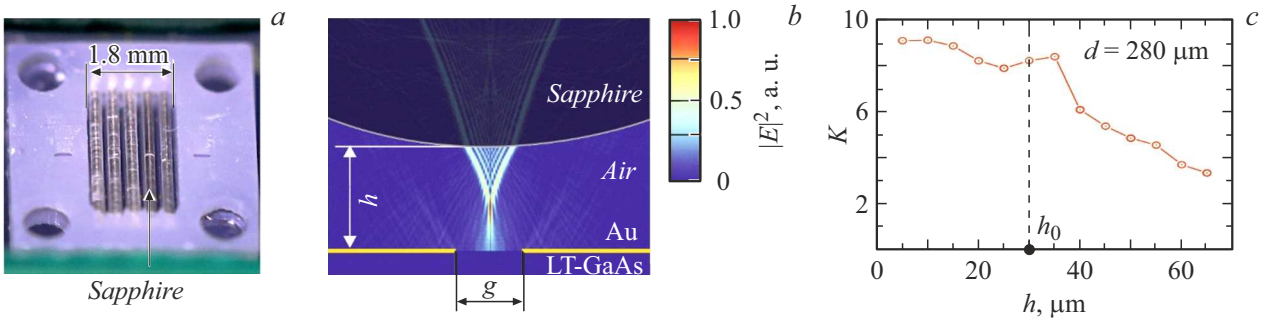

Figure 1. Concept of an LAPC emitter with SSF. *a* — Photographic image of the fabricated LAPC emitter containing five fibers; *b* — numerical model of pumping of a single strip emitter through SSF for air gap h optimization (the pattern of distribution of laser excitation $\sim |E|^2$ with fiber corresponds to $h_0 = 30\,\mu$m); and *c* — excitation power gain $K(h)$ calculated for different air gap values.

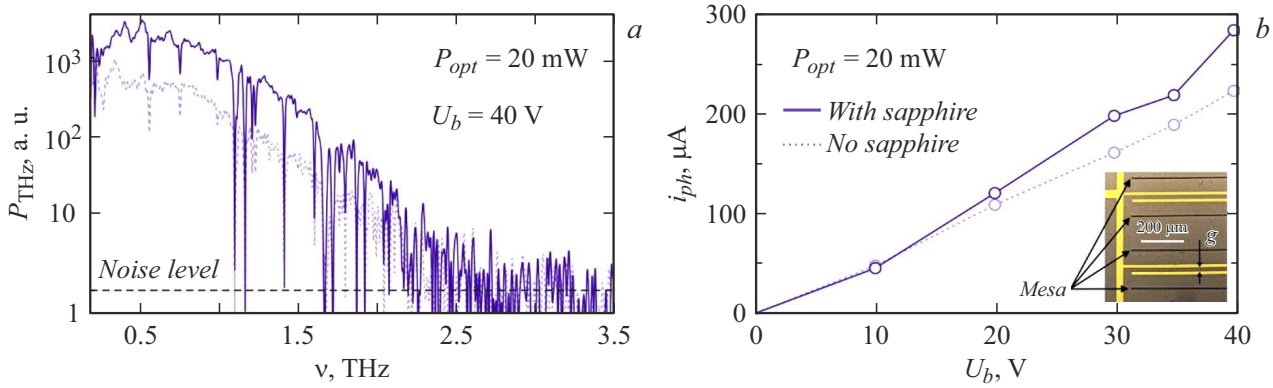

Figure 2. Experimental testing of the LAPC emitter. Comparative spectra of THz emission (*a*) and average photocurrents i_{ph} (*b*) for the LAPC emitter with SSF (solid curve) and without fibers (dashed curve). The inset presents a microscopic image of a section of the photoconductor surface with electrodes. *Mesa* — etched mesa structure in the photoconductor.

LAPC emitter, which was lacking in the original theoretical concept. Calculations of the spatial distributions of laser excitation power $\sim |E|^2$ with different parameters h for SSF with diameter $d = 280\,\mu$m (Fig. 1, *b*) were carried out by solving the Maxwell's equations numerically in COMSOL Multiphysics™. Following [4], we then integrated the values of $|E|^2$ over interelectrode gap g. An LT-GaAs layer grown by molecular beam epitaxy, where the carrier drift length was $\sim 1.0\,\mu$m, was chosen as a photoconductor. The calculated $K(h)$ dependence shown in Fig. 1, *c* was used to choose air gap $h_0 \approx 30\,\mu$m for 3D printing of the fixture. It can be seen that the calculated parameter h_0 provides $K \approx 8.2$.

Two LAPC emitter prototypes were fabricated for comparative analysis: one with the fixture with SSF and the other without fibers. The LAPC emitter prototypes were examined using a pulsed THz spectrometer based on an Avesta EFOA-SH femtosecond fiber laser with a wavelength of 780 nm, a pulse duration of ~ 100 fs, and a pulse repetition rate of 70 MHz [8]. The laser beam was split into two beams: one for excitation of samples and another for probing a TERA-8 photoconductive detector (Menlo Systems, Germany). The average laser excitation power of the LAPC emitter was just $P_{opt} = 20$ mW. Since the laser beam diameter was $(1/e^2) \sim 1.5$ mm, it was focused into an elliptical spot on the surface of the prototypes by a long-focus cylindrical lens to eliminate unwanted losses. The bias voltage of the LAPC emitter had a square waveform with a frequency of 20 kHz and amplitude $U_b = 40$ V. Two hyperhemispherical silicon lenses with a diameter of 12 mm were used for matching the source and detector of THz radiation with free space. Average photocurrent i_{ph} for the LAPC emitter prototypes was measured by the voltage drop across a 500 Ω resistor.

Figure 2, *a* shows the experimental spectra of THz radiation from the LAPC emitter with SSF and without fibers. It is evident that the near-field confinement of laser excitation near the edges of electrodes induced by SSF does not affect the shape and width of the spectrum, but provides a $\simeq$ 5-fold increase in THz power (an added 6.5 dB to the signal-to-noise ratio), which correlates well with the simulation results presented in Fig. 1, *c*. Figure 2, *b* presents the dependences of photocurrent i_{ph} for the LAPC emitter with SSF and without fibers on bias voltage U_b. It can be seen that the curves are virtually matching at low bias, but start to deviate at $U_b > 13$ V. This may be

attributed to a certain inaccuracy in the placement of SSF in the cells, which leads to a shift of the regions of laser excitation confinement relative to the edges of electrodes. In this case, a stronger electric bias field increases the effective drift length of carriers, facilitating their reaching the electrodes (i. e., it alleviates the error of SSF placement). At $U_b = 40$ V, the powers of THz radiation for LAPC emitters with SSF and without fibers differ by less than an order of magnitude (Fig. 2, *a*), which correlates with a $\simeq 30\,\%$ enhancement of photocurrent at the same bias voltage in Fig. 2, *b*.

Thus, an original approach aimed at confining laser excitation radiation in the LAPC emitter using an array of closely packed sapphire microlenses was verified experimentally. A $\simeq 5$-fold increase in THz radiation power, which raised the signal-to-noise ratio by 6.5 dB, was observed for a source with SSF. Note that the use of higher-power (e. g., Ti:Sapphire) lasers and the application of a higher bias voltage to the LAPC emitter electrodes may provide an additional several-fold enhancement of THz radiation power. Moreover, the proposed approach is easy to apply to large-area photoconductive THz detectors [9], which should help increase their sensitivity.

Funding

The work on design and fabrication of the LAPC emitter with SSF was supported financially as part of the state assignment of the National Research Center „Kurchatov Institute." The measurements of spectral characteristics of the LAPC emitter with and without fibers were supported by grant 25-79-30006 from the Russian Science Foundation.

Conflict of interest

The authors declare that they have no conflict of interest.

References

[1] M. Koch, D. Mittleman, J. Ornik, E. Castro-Camus, Nat. Rev. Meth. Primers, **3**, 48 (2023). DOI: 10.1038/s43586-023-00232-z
[2] D.S. Ponomarev, A.E. Yachmenev, D.V. Lavrukhin, R.A. Khabibullin, N.V. Chernomyrdin, I.E. Spektor, V.N. Kurlov, V.V. Kveder, K.I. Zaytsev, Phys. Usp., **67** (1), 3 (2024). DOI: 10.3367/UFNe.2023.07.039503.
[3] M.S. Vitiello, L. Viti, Appl. Phys. Rev., **12**, 011321 (2025). DOI: 10.1063/5.0199461
[4] D.S. Ponomarev, D.V. Lavrukhin, N.V. Zenchenko, I.A. Glinskiy, R.A. Khabibullin, V.N. Kurlov, K.I. Zaytsev, Tech. Phys. Lett., **48** (12), 8 (2022). DOI: 10.21883/TPL.2022.12.54936.19332.
[5] A. Singh, J. Li, A. Pashkin, R. Rana, S. Winnerl, M. Helm, H. Schneider, Opt. Express, **29** (13), 19920 (2021). DOI: 10.1364/OE.427247
[6] G.M. Katyba, K.I. Zaytsev, I.N. Dolganova, N.V. Chernomyrdin, V.E. Ulitko, S.N. Rossolenko, I.A. Shikunova, V.N. Kurlov, Prog. Cryst. Growth Charact. Mater., **67** (3), 100523 (2021). DOI: 10.1016/j.pcrysgrow.2021.100523
[7] D.S. Ponomarev, D.V. Lavrukhin, I.A. Glinskiy, A.E. Yachmenev, N.V. Zenchenko, R.A. Khabibullin, T. Otsuji, Yu. Goncharov, K.I. Zaytsev, Opt. Lett., **48** (5), 1220 (2023). DOI: 10.1364/OL.486431
[8] D.V. Lavrukhin, Yu.G. Goncharov, P.A. Khabibullin, K.I. Zaytsev, D.S. Ponomarev, Tech. Phys. Lett., **50** (4), 52 (2024). DOI: 10.61011/PJTF.2024.08.57513.19839.
[9] P.-K. Lu, D. Turan, M. Jarrahi, Opt. Express, **28**, 26324 (2020). DOI: 10.1364/OE.400380

Translated by D.Safin